

Journal of Materials Chemistry B

Accepted Manuscript



This is an *Accepted Manuscript*, which has been through the Royal Society of Chemistry peer review process and has been accepted for publication.

Accepted Manuscripts are published online shortly after acceptance, before technical editing, formatting and proof reading. Using this free service, authors can make their results available to the community, in citable form, before we publish the edited article. We will replace this *Accepted Manuscript* with the edited and formatted *Advance Article* as soon as it is available.

You can find more information about *Accepted Manuscripts* in the [Information for Authors](#).

Please note that technical editing may introduce minor changes to the text and/or graphics, which may alter content. The journal's standard [Terms & Conditions](#) and the [Ethical guidelines](#) still apply. In no event shall the Royal Society of Chemistry be held responsible for any errors or omissions in this *Accepted Manuscript* or any consequences arising from the use of any information it contains.

Submitted to Journal of Materials Chemistry B

A multi-functional polyhydroxybutyrate nanoparticle for theranostic applications

Hee-Su Kwon,^{a†} Sung-Geun Jung,^{a †‡} Hae-Yeong Kim,^a Stephanie A. Parker,^b Carl A. Batt^{bc}
and Young-Rok Kim^{a*}

^a *Institute of Life Sciences and Resources & Department of Food Science and Biotechnology,
College of Life Sciences, Kyung Hee University, Yongin, 446-701, Republic of Korea*

^b *Graduate field of Biomedical Engineering, Cornell University, Ithaca, NY 14850 USA*

^c *Department of Food Science, Cornell University, Ithaca, NY 14850 USA*

* Corresponding author: youngkim@khu.ac.kr, *Tel: +82-31-201-3830; Fax: +82-31-204-8116*

† These authors contributed equally to this work

‡ Present Address: LG Life Sciences, Immunodiagnostics Team, Daejeon, 305-380 Republic of Korea

Abstract

Biopolymer-based multifunctional nanoparticles were developed through one-step enzymatic polymerization reaction using engineered polyhydroxyalkanoate (PHA) synthase fused with green fluorescent protein (GFP) and a colon cancer-specific single chain variable fragment antibody (A33scFv). PHA synthase possesses unique catalytic characteristics, namely covalent catalysis, by which synthesized PHB chain remains covalently attached to the enzyme. The amphiphilic nature of resulting protein-polymer hybrid gave rise to a spontaneous self-assembly into a micellar structure with GFP and A33scFv displayed on the surface (AGPHB nanoparticle). A model compound, Nile-red, was loaded into the hydrophobic core of AGPHB nanoparticle during polymerization and self-assembly process. The specificity of the fluorescent multi-functional AGPHB nanoparticle toward colon cancer cell lines, SW1222 (A33+) and HT29 (A33-), was confirmed and analyzed quantitatively *in vitro*. This new biological approach will provides a fairly simple means of producing nanocarriers with a range of surface functionality and a desired sizes for imaging and targeted drug delivery.

Keywords

polyhydroxyalkanoate, polyhydroxybutyrate, enzymatic synthase, theragnosis, GFP, A33scFv, colon cancer.

Introduction

Polyhydroxyalkanoates (PHAs) are aliphatic polyesters produced by a wide range of microorganisms as intracellular carbon and energy storage compounds.¹ PHAs have gained particular interest since they were shown to be biodegradable and biocompatible.^{2,3} They have also been proposed as being fifth class of physiologically important organic biopolymer along with polynucleotides, polysaccharides, polypeptides and polyisoprenoids.⁴ A number of *in vitro* and *in vivo* tests have revealed that PHAs are compatible with bone, cartilage tissues, blood and various cell lines.⁵⁻¹¹ With these remarkable properties, PHAs have potential applications ranging from drug delivery to tissue engineering.⁶⁻¹³ The length of side chain and the functional groups in monomer determine the properties of PHAs, such as melting point, glass transition temperature, crystallinity and biodegradability.¹⁴ The most commonly found homopolymer of the PHA family is polyhydroxybutyrate (PHB), which has a methyl side chain. PHA synthase is the key enzyme that catalyse the polymerization of monomer, 3-(*R*)-hydroxybutyryl-coenzyme A (3HB-CoA), to PHB.¹⁵ PHA synthase has been known to catalyse the polymerization reaction *in vitro* and form PHB micelle.¹⁶⁻¹⁸ The polymerization reaction occurs through covalent catalysis, and thus the synthesized polymer chain is covalently attached to a specific amino acid residue, Cys₃₁₉, within the enzyme.¹⁹ The amphiphilic block copolymers of enzyme-PHB conjugate are consequently self-assembled into a micelle structure under aqueous conditions by hydrophobic interactions between the PHB chains. The enzymes on the surface of micelles are active and continue directing polymerization inward into the micelle displacing water from the vesicles.^{20, 21} The micelles are further stabilized by the hydrophilic protein block, PHA synthase, that faces into aqueous solution and form the hydrated shell. Hydrophobic small molecules have shown to be incorporated into the hydrophobic core of PHB micelle spontaneously during polymerization reaction.¹⁸ In addition, amino- or carboxy-terminal of the PHA synthase could be engineered through recombination technology to have a specific ligand, such as RGD4C (Cys-Asp-Cys-Arg-Gly-Asp-Cys-Phe-Cys), for synthesizing PHB nanocarrier with a targeting capability toward tumor cells that overexpress integrin.^{18, 22}

In this study, PHA synthase fused with antigen binding domain of monoclonal antibody A33 (A33scFv) and green fluorescent protein (GFP) was constructed for the synthesis of theranostic nanocarrier that can deliver a model drug to target cell and label the cell at the same time through the specific ligand-receptor action of A33scFv and fluorescent nature of GFP. The

monoclonal antibody (mAb) A33 is specific to a membrane antigen that is expressed in >95% of human colon cancers but absent in most human normal tissues and other tumor types.²³ Although mAb A33 is useful for detecting A33 positive cancer cell lines, it can be degraded and cleared easily by the body system. This limitation has been overcome using a small antigen binding domain, a single chain variable fragment (A33 scFv), without affecting the binding ability.²⁴ Here we expressed the recombinant tri-fusion protein (A33scFv-GFP-PHA synthase, AGP synthase) from *E. coli* through a protein engineering technique. Purified AGP synthase retained its catalytic activity and successfully synthesized the fluorescent PHB nanocarrier having a specific affinity toward human colon cancer cells through one step enzymatic reaction in an aqueous solution. The specificity and efficiency of the multi-functional PHB nanocarrier with A33scFv and GFP on the surface (AGPHB nanoparticle) were verified using A33-positive colon cancer cell line, SW1222, and A33-negative cell line, HT29, *in vitro*.

Experimental section

Materials

pET21a (Novagen, Madison, WI, USA) and pMAL-c2X (New England Biolabs, Ipswich, MA, USA) were used as expression vectors for AGP synthase and A33scFv, respectively. The host microorganisms for sub-cloning and protein expression were *Escherichia coli* DH10B (Invitrogen, Carlsbad, CA, USA) and *E. coli* Rosetta-gamiTM (Novagen, Madison, WI, USA), respectively. The colon cancer cell lines, SW1222 (Ludwig Institute for cancer Research, New York, NY, USA) and HT29 (American Type Culture Collection, Manassas, VA, USA) were used for the *in vitro* targeting assay. DL- β -hydroxybutyryl coenzyme A (3HB-CoA), Isopropyl- β -D-thiogalactopyranoside (IPTG), ethylenediaminetetraacetic acid (EDTA) and 5,5'-dithiobis(2-nitrobenzoic acid) (DTNB) were purchased from Sigma-Aldrich (St. Louis, MO, USA).

Construction of recombinant gene

To prepare AGP synthase, the genes encoding A33scFv and GFP were fused to the upstream of the *phaC* gene from *Cupriavidus necator*. To minimize steric hindrance and subsequent functional deterioration of fused proteins, the 15 amino acids flexible linker (LGGGGSGGGGSAA) was introduced between A33scFv and GFP. The primers for A33scFv forward (5'-CCG GAA TTC ATG GAG CTG CAG ATG ACC ACC CAG-3'), A33scFv

reverse (5'-AGA ACC ACC ACC ACC AGA ACC ACC ACC ACC CAG AGA GGA GAC GGT GAC CAG GT-3'), *gfp* forward (5'-GGT GGT TCT GGT GGT GGT GGT TCT GCG GCG GCG CGT AAA GGA GAA GAA CTT TTC-3'), *gfp* reverse (5'-GCC TTT TCC GGT CGC TTT GTA TAG TTC ATC CA-3'), *phaC* forward (5'-GTC ACC GTC TCC TCT GCG ACC GGA AAA GGC GCG-3') and *phaC* reverse (5'-CCG CTC GAG TGC CTT GGC TTT GAC GTA TCG CCC-3') were used in three sets of PCRs to amplify the DNA fragments of *A33scFv* (756 bp), *gfp* (714 bp) and *phaC* (1764 bp), respectively. These DNA fragments were annealed at their overlapping region and amplified by PCR. The fused DNA fragment (*A33scFv-gfp-phaC*, 3279 bp, included 45 bp of linker sequence) was purified using a gel extraction kit and digested with *EcoRI* and *XhoI* to ligate into an expression vector, pET21a. All PCRs were performed in a 30 µl reaction volume containing 0.75 unit Taq polymerase, 0.2 mM dNTP, 2 mM MgCl₂, 50 ng of template DNA, 0.33 µM of primer (forward and reverse) for 20 cycles. The extension times for *A33scFv*, *gfp*, *phaC*, *A33scFv-gfp* and *A33scFv-gfp-phaC* were 1, 1, 1.5, 2.5 and 3.5 min, respectively. For the competition assay, free *A33scFv* was expressed from *E.coli* Rosetta-gamiTM harbouring *A33scFv/pMAL-c2X*. The primers for *A33scFv* forward (5'-CCG GAA TTC ATG GAG CTG CAG ATG ACC ACC CAG-3'), *A33scFv* reverse (5'-CCC AAG CTT GTG GTG GTG GTG GTG GTG AGA GGA GAC GGT GAC CAG-3') were used to amplify the *A33scFv* gene (756 bp), which was digested with *HindIII* and *EcoRI*, and then ligated into the corresponding sites of pMAL-c2x.

Expression and purification of recombinant proteins

For the expression of AGP synthase and *A33scFv*, *E.coli* Rosetta-gamiTM was transformed with pET21a/*A33scFv-gfp-phaC* and pMAL-c2X/*A33scFv*, respectively. The transformed *E.coli* was grown aerobically at 37°C with constant shaking in Luria Bertani (LB) medium containing ampicillin (100 µg/ml) or chloramphenicol (25 µg/ml). The culture was incubated to an optical density of 0.5 at 600 nm. The culture was induced by the addition of 1.0 mM IPTG and was grown at 15°C with constant shaking at 200 rpm. After 24 hrs induction, the cultures were harvested by centrifugation, and the proteins were purified using Ni-NTA agarose resin (QIAGEN, Hilden, Germany) and amylose resin (New England Biolabs, Ipswich, MA, USA) according to the manufacturer's instructions. The protein concentration was determined using the Bradford method with bovine serum albumin (BSA) as the standard. The molecular sizes of purified proteins were confirmed by 10% sodium dodecyl sulfate-polyacrylamide gel

electrophoresis (SDS-PAGE) and Coomassie brilliant blue staining (Bio-Rad, Hercules, CA, USA). The expressed proteins were confirmed further by a western blot assay. The proteins were electrophoresed on 10% SDS-PAGE and electroblotted onto a nitrocellulose membrane (Whatman, Dassel, Germany). To identify the native and tri-fusion AGP synthase, the electroblotted membrane was incubated with the HRP-conjugated anti-His₆-antibody (Roche, Mannheim, Germany). Non-radioactive detection was carried out using the protocol provided from the Immun-Star HRP chemiluminescence detection kit (Bio-Rad, Hercules, CA, USA).

Synthesis and size analysis of PHB nanoparticles

The polymerization reaction was carried out in a 20 mM potassium phosphate buffer (pH 7.0) containing 200 mM NaCl, 5 mM 3HB-CoA, and various concentration of native PHA synthase (72.2 nM, 288 nM, 1,155 nM, 4,621 nM, 18,484 nM, 73,936 nM, 147,873 nM) at 37 °C for 1 hr. The sizes of PHB nanoparticles were examined using dynamic light scattering (DLS, ELS-Z2, OTSUKA, JAPAN) with a laser wavelength of 638 nm and a scattering angle of 165 °. Before measurement, the synthesized PHB nanoparticles were resuspended in a 1ml of deionized water. The morphology of PHB nanoparticle was analyzed by Field emission scanning electron microscope (FE-SEM, LEO SUPRA 55, Carl Zeiss, Germany) at 5 kV. For FE-SEM analysis, a 10 µl of the solution containing PHB nanoparticle was applied onto the surface of Si-wafer that was thoroughly cleaned with ethanol followed by O₂ plasma cleaning. Once the solution was dried the Si-wafer was rinsed with deionized water to remove remaining salt crystals. The samples were put on a desiccator for 24 hrs before FE-SEM analysis.

Synthesis and characterization of AGPHB nanoparticle

The polymerization reaction was carried out in 20 mM potassium phosphate buffer (pH 7.0) containing 200 mM NaCl, 5 mM 3HB-CoA, and 1.5 µM enzymes at room temperature. The activities of native PHA synthase and AGP synthase were determined using an Ellman's assay, which measures the free thiols released during the polymerization reaction.²⁵ A 10 µl aliquot of the reaction mixture was taken every 2 min and mixed with 390 µl of a 0.5 mM sodium acetate buffer (pH 4.7) containing 50 mM NaCl and 0.5 mM EDTA. A total of 690 µl of 40 mM sodium phosphate buffer (pH 7.6) containing 2 mM EDTA and 10 µl of 100 mM DTNB were then added and mixed at room temperature for 1 min. The absorbance of the solution was measured spectrophotometrically at 412 nm using water as the control. The molar extinction

coefficient ($\text{cm}^{-1} \text{M}^{-1}$) of DTNB in reacting with free thiol was 13,600. The enzymatically synthesized PHB nanoparticles were analysed by DLS and FE-SEM as described above. The polymerization reaction was carried out at the same condition for 2 hrs for both analysis.

Tumor cell targeting assay

SW1222 and HT29 colon cancer cells were selected as the antigen positive (A33+) and negative (A33-) cells, respectively. All cells were grown in DMEM medium (Welgene, Korea) supplemented with 10% heat-inactivated fetal bovine serum (FBS), penicillin (100 U/ml) and streptomycin (100 mg/ml) at 37°C in a humidified atmosphere containing 5% CO₂. To examine the targeting ability, the AGPHB nanoparticles were synthesized by AGP synthase with 1% Nile red (0.15 mg Nile red/ml in dimethylsulfoxide) in the same reaction mixture. The excitation and emission wavelengths of Nile red were 513-530 nm and 525-605 nm, respectively. The excess Nile red was removed and the synthesized nanoparticles were collected by centrifugation at 10,000 rpm for 10 min followed by washing five times with DMEM medium. The trypsinized SW1222 and HT29 cells were resuspended in serum-free media and plated onto flat-bottom 96-well plates at a density of 1×10^4 cells per well. After 24 hrs incubation, the enzymatically-synthesized AGPHB nanoparticles were added to each culture well. The treated SW1222 and HT29 cells were incubated for 2 hrs in a CO₂ incubator at 37°C. The unbound nanoparticles were removed by careful washing with PBS three times. The cells were then observed by a Nikon TE2000 inverted fluorescence microscope.

Competition assay

For the competition assay, the SW1222 cells were plated and grown onto flat-bottom 96-well plates at a density of 1×10^4 cells per well. Before adding the enzymatically synthesized AGPHB nanoparticles, the SW1222 cells were pre-incubated with various concentrations of free A33scFv (15, 90, 185 and 315 μM) for 2 hrs in a 5% CO₂ incubator at 37°C. The unbound A33scFv was removed by washing three times with 200 μl of Hank's balanced salt solution (HBSS). The cells were then treated with the enzymatically synthesized AGPHB nanoparticles for 2 hrs and the unbound nanoparticles were removed by washing three times with 200 μl of HBSS. The fluorescence signal from the AGPHB nanoparticles attached to the target cell was measured using a fluorescence microplate reader (Infinite 200, TECAN, Mannedorf, Switzerland) with excitation and emission wavelength of 485 nm and 530 nm, respectively.

Results and discussion

This paper reports an enzymatically synthesised multifunctional nanoparticle using PHA synthase fused with GFP and A33scFv and its application in both imaging and targeted drug delivery. Fig 1 shows the overall scheme of enzymatic synthesis of the AGPHB nanoparticle. PHA synthase catalyzes the polymerization of the 3HB-CoA substrate to PHB. Because the polymerization reaction occurs through covalent catalysis, the synthesized polymer chain remains bound covalently to a specific amino acid residue within the enzyme.^{19, 26} The covalent linkage between the hydrophilic tri-fusion proteins and hydrophobic polymer chain results in the formation of an amphiphilic block copolymer that is spontaneously self-assembled into a micellar structure under aqueous conditions. Hydrophobic drugs or active agents can be incorporated into the core of the micelle during the polymerization and self-assembly steps. The A33scFv/GFP moiety fused with PHA synthase is displayed on the surface of the micelle and confers targeting and fluorescent properties to the AGPHB nanoparticle.

To produce the AGP synthase, the genes encoding A33scFv and GFP were ligated into the upstream of the *phaC* gene encoding PHA synthase, as described in the experimental section. The fused DNA fragment (3279 bp) was inserted into an expression vector, pET21a, flanked by *EcoRI* and *XhoI*. This construct was transferred to *E. coli* Rogetta-gami (DE3) for overexpression. The AGP synthase was purified under native condition and analysed by SDS-polyacrylamide gel electrophoresis and a western blot assay (Fig 2). As expected, the size of AGP synthase was 118 kDa, whereas that of the native PHA synthase was 65 kDa. The catalytic activity of PHA synthase and the functions of two other moieties, A33scFv and GFP, were not much affected after being expressed as the fused form. The catalytic activity of PHA synthase was measured using Ellman's assay, which monitors the level of free thiols generated from the polymerization reaction.²⁵ The polymerization rate was slightly lower for AGP synthase compared to the native one (Fig 3a). The additional motives, A33scFv and GFP, which were introduced into the N-terminus of PHA synthase, had a slight effect on the catalytic activity of PHA synthase. The two additional motives are believed to have lowered the diffusion rate of the enzyme in an aqueous solution and also conferred steric hindrance to the dimerization site of the enzyme. PHA synthase from *Cupriavidus necator* is known to be active as a dimer form.^{19, 27} Therefore the lower polymerization activity observed at the early stage could be derived from slow dimerization of the fused enzyme. On the other hand, the full conversion of

monomers to polymer was achieved after approximately 30 min. The size and morphology of the PHB nanoparticles produced by native and AGP synthase under the same conditions were all fairly homogeneous (Fig 3b-c). According to the dynamic light scattering measurements, the average diameters of the PHB nanoparticles produced by native and AGP synthase were 219 ± 26 nm and 241 ± 39 nm, respectively. The size difference may be attributed to the larger molecular weight of AGP synthase (116 kDa) compared with native PHA synthase (65 kDa) because the proteins are displayed on the exterior of the nanoparticles. The nanoparticle was formed by the spontaneous aggregation of hydrophobic PHB blocks to minimize its contact with the surrounding aqueous solution. The aggregate was stabilized further by the hydrophilic protein blocks that face toward the aqueous solution and formed a hydrated shell. GFP and A33scFv are displayed on the surface of the PHB nanoparticle along with PHA synthase, conferring fluorescent and targeting ability to the resulting nanoparticle.

The specific binding affinity of the enzymatically synthesized AGPHB nanoparticle for tumor cells was determined using SW1222 (A33+) and HT29 (A33-) colon cancer cell lines. The A33 antigen is expressed in 95% of human colorectal cancer, such as the SW1222 human colon cancer cell line. For the targeting experiment, AGPHB nanoparticles were synthesized using AGP synthase with 1% Nile red in the same reaction mixture. Nile red was used as a model drug, which is incorporated into the hydrophobic core of the PHB nanoparticle during polymerization reaction. The resulting AGPHB nanoparticle that presents A33scFv and GFP on the surface was used to monitor the specific adhesion and uptake by the SW1222 human colon cancer cells. The SW1222 and HT29 cells were plated into flat-bottom 96-well plate. After incubating for 24 hrs, the cells were treated with the AGPHB nanoparticle for 2 hrs and washed three times with DPBS. The cells were then observed by fluorescence microscopy with the excitation and emission wavelength corresponding to GFP and Nile-red. The fluorescence micrographs confirmed that the AGPHB nanoparticles effectively target the A33 positive target cells, SW1222 (Fig 4). The GFP on the surface of the AGPHB nanoparticles gives a green colour, whereas Nile-red in the core imparts a red colour to the AGPHB nanoparticles. When two images for GFP and Nile red were superimposed, the staining pattern matched precisely, suggesting that AGPHB nanoparticles can be used to image target cells and deliver desired active compounds to the target cell at the same time (Fig 4d). On the other hand, there was no observable binding with the A33 negative cells, HT29, indicating that the A33scFv motif on the surface of AGPHB nanoparticle is solely responsible for the specificity of the nanocarrier

to the target cell (Fig 4f-g). In other words, the AGPHB nanoparticle is capable of targeting specific tumor cells that express the A33 antigen and being readily visualized by fluorescence devices. An inhibition assay was carried out using free A33scFv to confirm that the binding occurs through the specific affinity between the A33scFv moiety of the AGPHB nanoparticle and the A33 antigen displayed on the surface of the colon cancer cell. For the inhibition assay, the SW1222 cells were prepared the same way, as described above. Before applying the AGPHB nanoparticle, the cells were pre-incubated with various concentrations of free A33scFv (15 - 315 μM) for 2 hrs. The cells were then reacted with AGPHB nanoparticles for 2 hrs and the unbound nanoparticles were removed by washing three times with 200 μl of HBSS. The green fluorescence from the AGPHB nanoparticles that were bound to the target cells were measured using a fluorescence spectrophotometer with excitation and emission at 485 nm and 530 nm, respectively. The specific binding and internalization of the AGPHB nanoparticle to the A33 positive target cells, SW1222, was inhibited in the presence of free A33scFv in a concentration-dependent manner (Fig 5). The A33 antigens on the surface of target cells were preoccupied with the free A33scFv protein, which prevented the binding of AGPHB nanoparticles to the target cell. The binding of the AGF nanoparticles was blocked completely when the cells were treated with free A33scFv at a concentration of more than 200 μM . This clearly shows that the binding of AGP nanoparticles to the target cell occurs through a specific interaction between A33scFv on the AGPHB nanoparticle and the A33 antigen on the surface of human colon cancer cells.

The size of nanoparticle is one of the most important characteristics as a drug carriers along with the encapsulation efficiency and release characteristics. Small nanoparticles are easily removed by renal excretion system whereas large ones are caught by the mononuclear phagocytic system (MPS) cells in liver, spleen and bone marrow^{28, 29}. Because of the varying fenestration size of target organs, the size of nanoparticles is also important for effective and precise delivery of encapsulated drug to target site. The advantage of this system, enzymatic synthesis of PHB nanoparticle, is that the size of PHB nanoparticle can be controlled by modulating the enzyme-substrate ratio (Fig 6). The reactions were carried out with different concentration of PHA synthase from 72.2 nM to 147,873 nM at fixed substrate concentration of 5 mM, which resulted in the formation of PHB nanoparticles with an average diameter ranging from 550 nm to 70 nm (Fig 6-a). The size of synthesized PHB nanoparticle decreases upon increasing enzyme concentration. Assuming that all the substrate is evenly consumed by

enzymes present in the reaction, the length of polymer chain growing from the enzyme is inversely proportional to the concentration of enzyme. In other words, the number of substrate available to each enzyme is defined by the initial enzyme concentration. It is also interesting to note that the volume of PHB nanoparticles is closely related with the calculated volume ratio of single PHB-PHA synthase copolymer chain at given enzyme concentration (Fig 6-b). The theoretical volume of a single PHB-PHA synthase copolymer was calculated by adding up the volume of synthesized PHB chain and the covalently attached dimeric PHA synthase. The molecular weights of the hydroxybutyrate monomer unit and dimeric PHA synthase are 86.09 g/mol and $2 \times 69,248.57$ g/mol whereas the densities of those are 1.1086 g/ml³⁰ and 1.41 g/ml,³¹ respectively. The close relationship between the actual volume of PHB nanoparticle and the calculated volume ratio of a single PHB-PHA synthase copolymer at varying enzyme concentration indicates that one PHB nanoparticle is formed as a result of self-assembly of a finite number of PHB-PHA synthase copolymer. The ability to control the size of PHB nanoparticle by modulating the enzyme-substrate ratio will further fine tune the functionality of multi-functional nanocarrier.

Conclusion

A facile way of preparing theranostic materials for colon cancer was developed through one-step enzymatic synthesis in an aqueous solution using tri-fusion AGP synthase and the substrate, 3HB-CoA. The engineered tri-fusion protein successfully catalysed the synthesis of AGPHB nanoparticle with A33scFv and GFP displayed on the surface. The A33scFv and GFP moieties imparted targeting and imaging capability to the AGPHB nanoparticle. A drug or active compound can be loaded readily into the core of the AGPHB nanoparticle during the polymerization and self-assembly process. This new approach provides a promising means of producing nanocarriers with a range of surface functionality and a desired sizes for imaging and targeted drug delivery. Moreover, utilization of over 100 different types of monomers that can generate PHAs with different physicochemical properties together with custom designed end-functionalities will significantly expand its application spectrum as a multi-functional nanocarrier.

Acknowledgements

This study was supported by Basic Science Research Program through the National Research

Foundation of Korea (NRF) funded by the Ministry of Education, Science and Technology (2010-0002963).

References

1. A. J. Anderson and E. A. Dawes, *Microbiol Mol Biol Rev*, 1990, **54**, 450-472.
2. H. Brandl, R. Bachofen, J. Mayer and E. Wintermantel, *Canadian J Microbiol*, 1995, **41**, 143-153.
3. H. Brandl, R. A. Gross, R. W. Lenz and R. C. Fuller, *Adv. Biochem. Eng./Biotechnol.*, 1990, **41**, 77-93.
4. H. M. Mueller and D. Seebach, *Angew. Chem.*, 1993, **105**, 483-509.
5. Y. Tesema, D. Raghavan and J. Stubbs, *J. Appl. Polym. Sci.*, 2004, **93**, 2445-2453.
6. T. Shinoka, C. K. Breuer, R. E. Tanel, G. Zund, T. Miura, P. X. Ma, R. Langer, J. P. Vacanti and J. E. Mayer, Jr., *Annals of Thoracic Surgery*, 1995, **60**, S513-516.
7. T. Shinoka, D. Shum-Tim, P. X. Ma, R. E. Tanel, R. Langer, J. P. Vacanti and J. E. Mayer, Jr., *Circulation*, 1997, **96**, II-102-107.
8. R. Sodian, S. P. Hoerstrup, J. S. Sperling, D. P. Martin, S. Daebritz, J. E. Mayer Jr. and J. P. Vacanti, *ASAIO*, 2000, **46**, 107-110.
9. D. Sendil, I. Gursel, D. L. Wise and V. Hasirci, *J. Controlled Release*, 1999, **59**, 207-217.
10. P. A. Holmes, *Phys. Technol.*, 1985, **16**, 32-36.
11. N. R. Boeree, J. Dove, J. J. Cooper, J. Knowles and G. W. Hastings, *Biomater.*, 1993, **14**, 793-796.
12. C. W. Pouton and S. Akhtar, *Advanced Drug Delivery Reviews*, 1996, **18**, 133-162.
13. S. F. Williams, D. P. Martin, D. M. Horowitz and O. P. Peoples, *Int. J. Biol. Macromol.*, 1999, **25**, 111-121.
14. M. Zinn, B. Witholt and T. Egli, *Adv. Drug Delivery Rev.*, 2001, **53**, 5-21.
15. A. Steinbüchel and H. G. Schlegel, *Mol. Microbiol.*, 1991, **5**, 535-542.
16. T. U. Gerngross and D. P. Martin, *Proc. Natl. Acad. Sci. USA*, 1995, **92**, 6279-6283.
17. R. W. Lenz, C. Farcet, P. J. KDijkstra, S. Goodwin and S. Zhang, *Int. J. Biol. Macromol.*, 1999, **25**, 55-60.
18. H.-N. Kim, J. Lee, H.-Y. Kim and Y.-R. Kim, *Chem. Commun.*, 2009, 7104-7106.
19. J. Wodzinska, K. D. Snell, A. Rhomberg, A. J. Sinskey, K. Biemann and J. Stubbe, *J. Am. Chem. Soc.*, 1996, **118**, 6319-6320.
20. L. Jurasek, G. A. R. Nobes and R. H. Marchessault, *Macromol. Biosci.*, 2001, **1**, 258-265.
21. G. A. R. Nobes, L. Jurasek, R. H. Marchessault, D. P. Martin, J. L. Putaux and H. Chanzy, *Macromol. Rapid Commun.*, 2000, **21**, 77-84.
22. J. Lee, S.-G. Jung, C.-S. Park, H.-Y. Kim, C. A. Batt and Y.-R. Kim, *Bioorg. Med. Chem. Lett.*, 2011, **21**, 2941-2944.
23. P. Garin-Chesa, J. Sakamoto, S. Welt, F. X. Real, W. J. Rettig and L. J. Old, *Int. J. Oncol.*, 1996, **9**, 465-471.
24. P. M. Deckert, C. Renner, L. S. Cohen, A. Jungbluth, G. Ritter, J. R. Bertino, L. J. Old and S. Welt, *Brit. J. Cancer*, 2003, **88**, 937-939.
25. R. Singh, W. A. Blattler and A. R. Collinson, *Anal. Biochem.*, 1993, **213**, 49-56.
26. Y.-R. Kim, H.-j. Paik, G. W. Coates, C. K. Ober and C. A. Batt, *Biomacromol.*, 2004, **5**, 889-894.
27. S. Zhang, T. Yasuo, R. W. Lenz and S. Goodwin, *Biomacromol.*, 2000, **1**, 244-251.

28. S. M. Moghimi, A. C. Hunter and J. C. Murray, *Pharmacological reviews*, 2001, **53**, 283-318.
29. R. Nakaoka, Y. Tabata, T. Yamaoka and Y. Ikada, *Journal of controlled release*, 1997, **46**, 253-261.
30. J. Mas, C. Pedros-Alio and R. Guerrero, *Journal of Bacterology*, 1985, **164**, 749-756.
31. H. Fischer, I. Polikarpov and A. F. Craievich, *Protein Science*, 2004, **13**, 2825-2828.

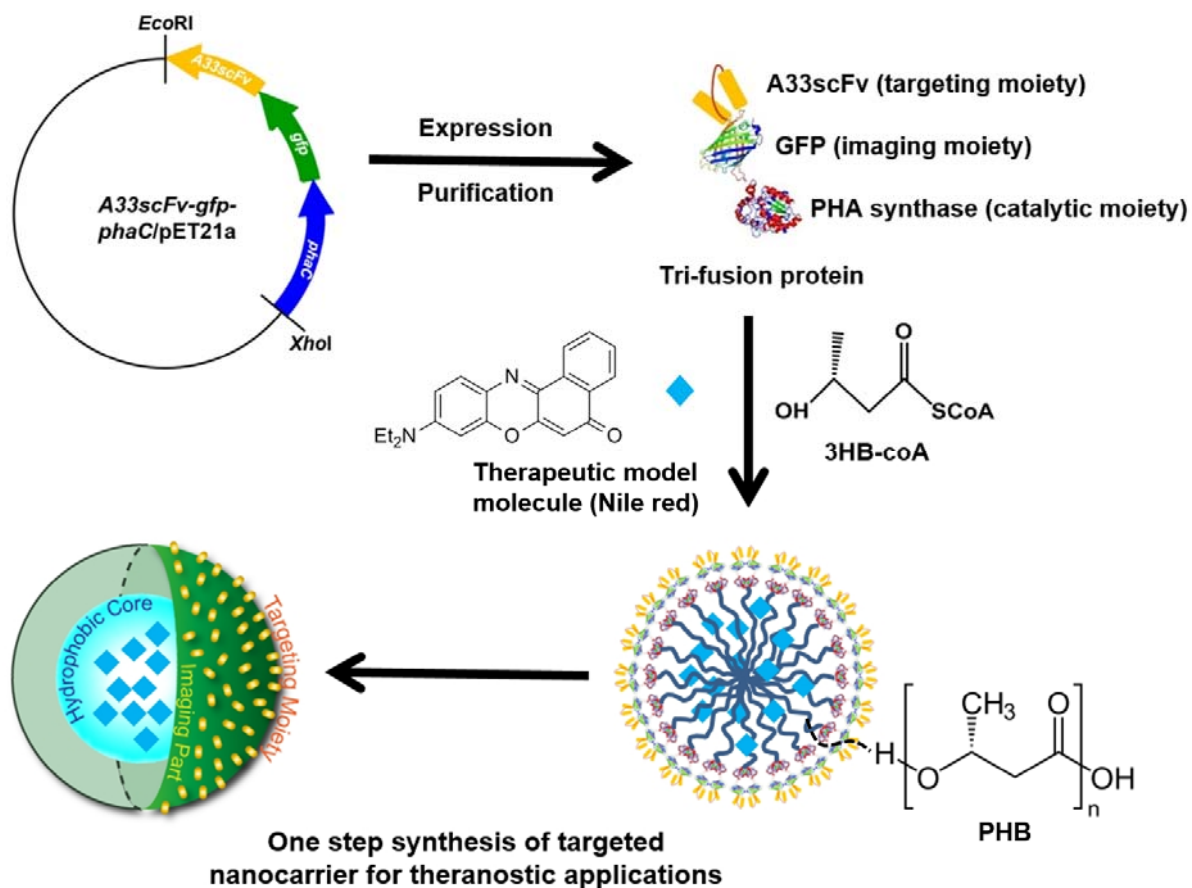


Figure 1 Schematic diagram representing the synthesis of theranostic PHB nanoparticles using AGP synthase. The fused enzyme is expressed from *E. coli* harbouring the engineered tri-fusion gene of *A33scFv*, *gfp* and *phaC*. First, a protein-PHB hybrid block copolymer was formed through a catalytic reaction of AGP synthase and substrate, 3HB-CoA. The hybrid block copolymer was then self-assembled into a micellar structure with GFP and A33scFv displayed on the surface, whereas hydrophobic therapeutic molecules were loaded into the core of the micelle during the self-assembly process.

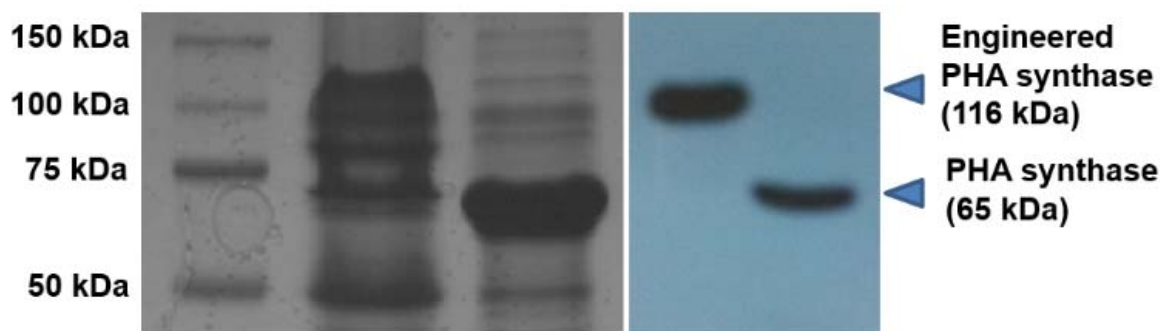


Figure 2 SDS-PAGE (left) and western blotting analysis (right) of native PHA synthase and engineered AGP synthase. The increased size of the AGP synthase (116 kDa) was derived from the co-expression of A33scFv and GFP together with PHA synthase in fused form. Western blotting analysis was performed using the anti-Histag antibody because the proteins are expressed with His(6)-tags in their N-terminus.

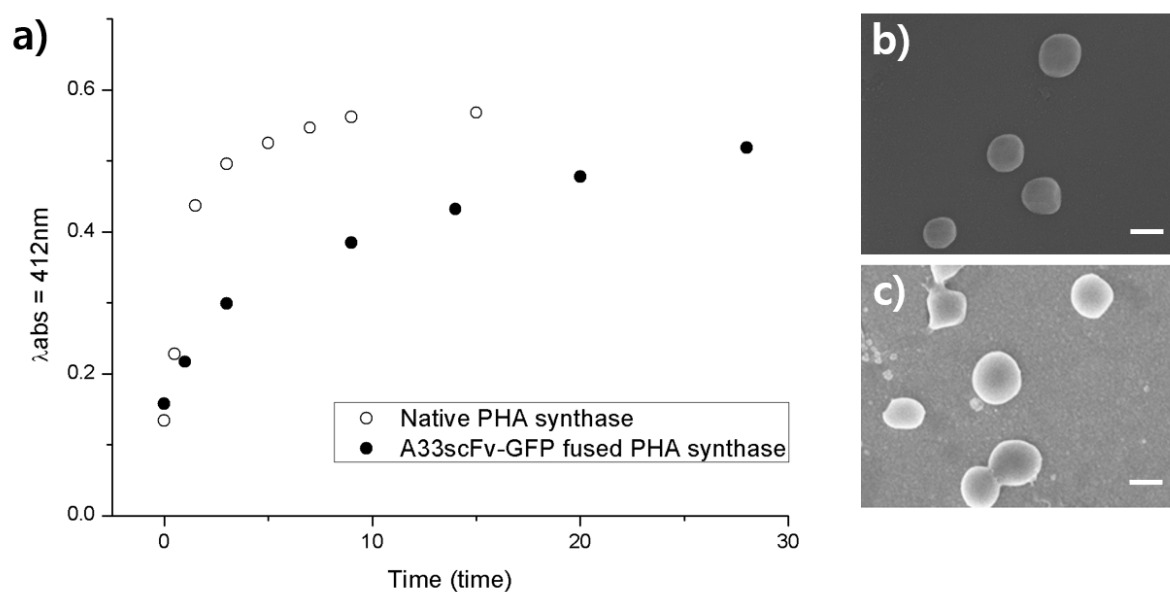


Figure 3 Analysis of Ellman's assay showing the activity of native PHA synthase and AGP synthase (a). FE-SEM images of synthesized PHB nanoparticles with native PHA synthase (b) and AGP synthase (c). Scale bar is 200 nm.

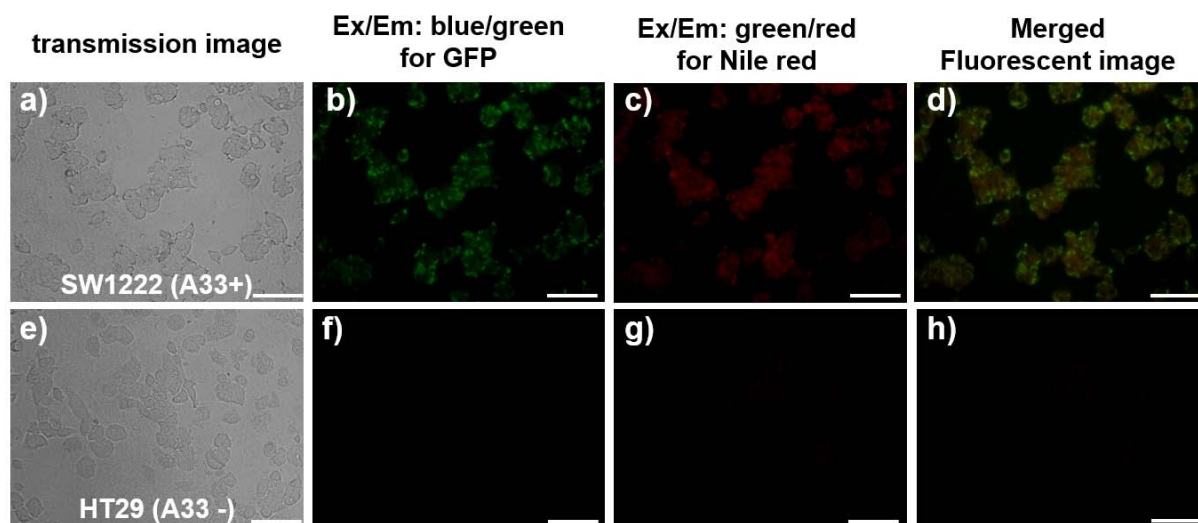


Figure 4 Transmission and fluorescence images of A33 antigen positive SW1222 (a-d) and A33 negative HT29 (e-h) colon cancer cells after being treated with the AGPHB nanoparticles loaded with Nile-red. The AGPHB nanoparticle binds specifically to the A33 antigen positive SW1222 cancer cells whereas its binding to the A33 negative HT29 cells was not detectable. The green and red fluorescence is from the GFP displayed on the surface of the AGP nanoparticle and the Nile-red loaded on the core of the AGP nanoparticle. The scale bar is 30 μm .

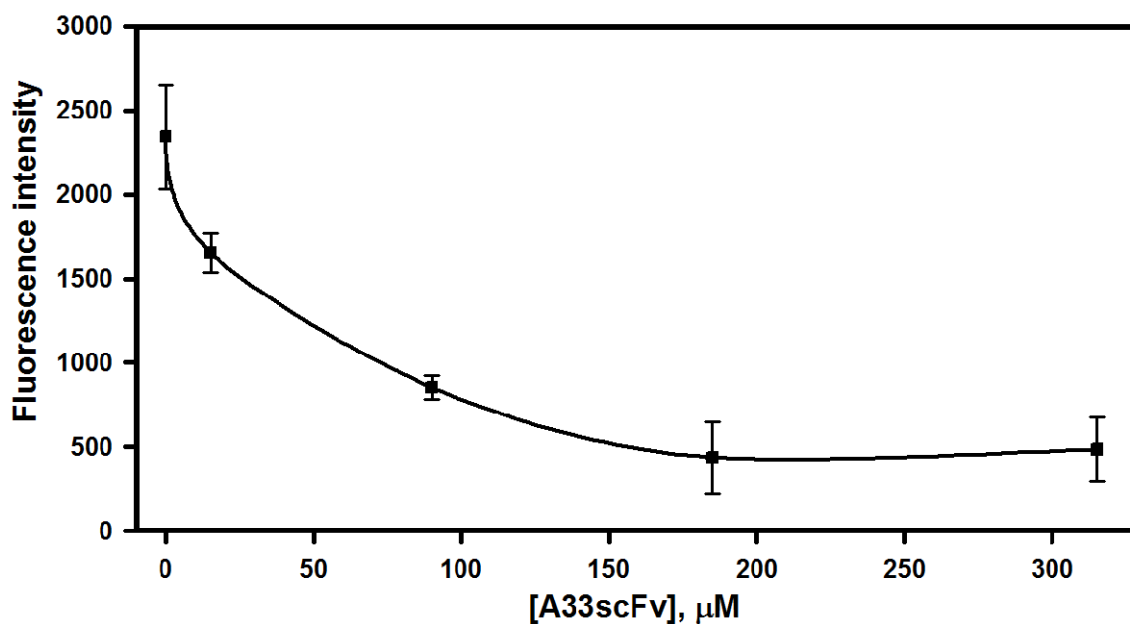


Figure 5 Inhibition of AGPHB nanoparticle binding to the target cell, SW1222, in the presence of various concentrations of free A33scFv protein. The fluorescence intensity from the AGPHB nanoparticles that are bound to the target cells being treated with free A33scFv protein was measured using a fluorescence spectrophotometer with excitation and emission at 485 nm and 530 nm, respectively. The figure is displayed with standard deviation as error bar from three independent experiments.

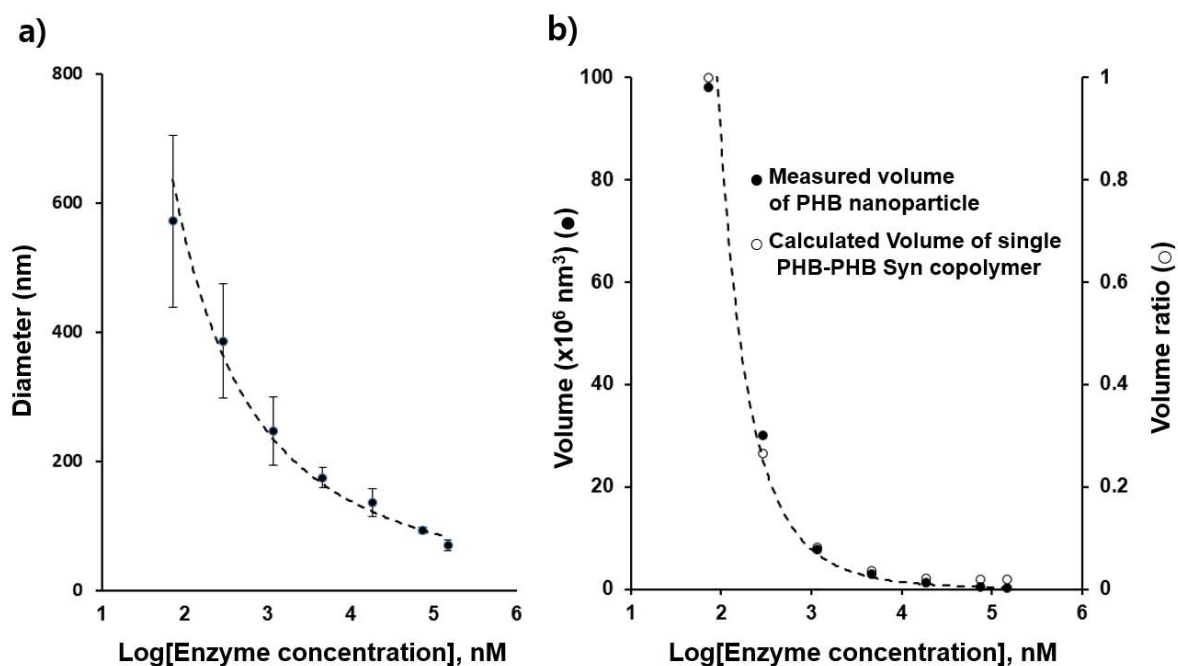


Figure 6 Average diameter (a) and volume (b) of PHB nanoparticle formed with 5 mM 3HB-CoA and varying enzyme concentration (72.2 nM, 288 nM, 1,155 nM, 4,621 nM, 18,484 nM, 73,936 nM and 147,873 nM). The figure is displayed with standard deviation as error bar from three independent experiments. (b), The correlation between the volume of a PHB nanoparticle (●) and calculated volume ratio of a single PHB-PHA synthase copolymer (○) at given enzyme concentration implies that a PHB nanoparticle is composed of a finite number of PHB-PHA synthase copolymer chains.